Applied Catalysis A: General 350 (2008) 178–185

Contents lists available at ScienceDirect

Applied Catalysis A: General

journal homepage: www.elsevier.com/locate/apcata

On the synthesis of $LaCl_3$ catalysts for oxidative chlorination of methane

Elvira Peringer, Chirag Tejuja, Michael Salzinger, Angeliki A. Lemonidou [1], Johannes A. Lercher *

Department of Chemistry, Technische Universität München, Lichtenbergstr. 4, D-85747 Garching, Germany

ARTICLE INFO

Article history:
Received 20 June 2008
Received in revised form 7 August 2008
Accepted 8 August 2008
Available online 15 August 2008

Keywords:
Methane
Oxidative chlorination
Hypochlorite anion
$LaCl_3$
LaOCl
Template synthesis

ABSTRACT

$LaCl_3$ is an active and selective catalyst for oxidative chlorination of methane to methyl chloride, generated in situ by chlorination from LaOCl. The latter is prepared by precipitation of $La(OH)_2Cl$ and subsequent calcination. The synthesis route was modified by using different bases in order to synthesize high surface area LaOCl catalyst precursors. Ammonium hydroxide and the organic bases tetraethylammonium hydroxide, tetrapropylammonium hydroxide, and tetrabutylammonium hydroxide are used as precipitating agents. The marked increase of the specific surface area by using organic bases indicates also that they may act as templating agents. After chlorination the specific surface areas of pure LaOCl samples decrease drastically, lanthanum carbonate, however, acts as structural promoter stabilizing the specific surface area during chlorination.

1. Introduction

$LaCl_3$ has been shown to be a highly stable and selective catalyst for oxidative chlorination of methane with hydrogen chloride and oxygen to methyl chloride and water (Eq. (1)) [1–3].

$$CH_4 + HCl + 0.5O_2 \rightarrow CH_3Cl + H_2O \quad (1)$$

The oxidative chlorination of methane with $LaCl_3$ has been concluded to be a surface catalyzed reaction with a transient hypochlorite species as the active site on the surface [2]. This hypochlorite species is formed by dissociative adsorption of oxygen on the surface. Methane reacts with the hypochlorite and forms a carbonium ion, followed by an exchange of hydrogen with the positively charged chlorine atom, creating a hydroxy group and a chloride vacancy. Hydrogen chloride is regenerating the surface via addition of Cl^- and the formation of water. This mechanism (see Fig. 1) is in line with the results of exploring the corresponding intermediates by DFT calculations [4,5].

The catalyst and the reaction route are advantageous compared to the well-known copper based catalysts which catalyze the Deacon reaction, the oxidation of hydrogen chloride and oxygen to chlorine gas. Methane is, thus, chlorinated via a gas-phase radical reaction with low selectivity towards methyl chloride over copper catalysts. Unlike the radical gas-phase chemistry of the copper catalyst, the surface catalyzed reaction over $LaCl_3$ provides the possibility to change activity and selectivity by modification of the catalyst, e.g., by changing the synthesis route. Van der Heijden et al. showed recently that the activity of $LaCl_3$ in the catalytic hydrogen–chlorine exchange between CCl_4 and CH_2Cl_2 can be greatly increased by increasing its specific surface by supporting it on CNF [6]. It should be noted however, that the carbon support prevents the use of such materials in oxidizing atmosphere at high temperatures.

$LaCl_3$ is a highly hygroscopic material and has to be prepared in situ. Dehydrated $LaCl_3$ can be generated by thermal transformation of lanthanum chloride heptahydrate in inert gas or hydrogen chloride. However, the dehydration has to proceed very slowly in order to avoid the transformation to LaOCl. Such commercially available $LaCl_3$ material possesses low specific surface areas.

A conceptually better route to materials with a high specific surface area is therefore the in situ chlorination of lanthanum oxychloride at 400 °C with hydrogen chloride. Lanthanum oxychloride is not hygroscopic and is stable when exposed to air.

Several synthesis routes to prepare LaOCl are known based on various ways to introduce the chlorine atom in the structure. The synthesis routes include the solid state reaction of lanthanum oxide with ammonium chloride at 1000 °C (Eqs. (2–4)) [7,8]. The reaction proceeds over a lanthanum chloride ammonia adduct and

* Corresponding author. Tel.: +49 89 289 13540; fax: +49 89 289 13544.
E-mail address: johannes.lercher@ch.tum.de (J.A. Lercher).
[1] On leave from the Department of Chemical Engineering, Aristotle University Thessaloniki, POB 1517, GR-54006 Thessaloniki, Greece.

0926-860X/$ – see front matter © 2008 Published by Elsevier B.V.
doi:10.1016/j.apcata.2008.08.009

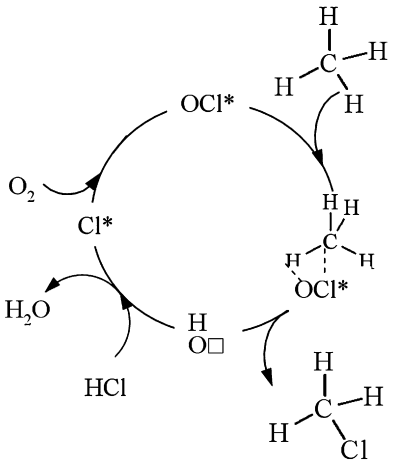

Fig. 1. Proposed reaction mechanism for oxidative chlorination of methane over $LaCl_3$-based catalysts [2].

the overall reaction is presented in Eq. (4).

$$La_2O_3 + 6NH_4Cl \rightarrow 2LaCl_3{\cdot}3NH_3 + 3H_2O \quad (2)$$

$$LaCl_3{\cdot}3NH_3 + La_2O_3 \rightarrow 3LaOCl + 3NH_3 \quad (3)$$

$$La_2O_3 + 2NH_4Cl \rightarrow 2LaOCl + 2NH_3 + H_2O \quad (4)$$

LaOCl can also be synthesized from lanthanum oxide and lanthanum chloride at room temperature via a mechano-chemical synthesis (Eq. (5)), but the upper limits of the specific surface area reachable is rather low for such approaches (1 m^2/g) [4,9].

$$La_2O_3 + LaCl_3 \rightarrow 3LaOCl \quad (5)$$

Marsal et al. used a sol–gel route with acrylamide as macroscopic template. Acrylamide is forming a 3D network in which a solution of La and Cl ions is soaked [10,11]. The gel is first dried in a microwave, followed by thermal treatment at 600 °C to obtain the final LaOCl powder. This method yields a homogenous distribution of faceted stick-shaped particles. The disadvantage of the solid state reactions is the required high temperature treatment leading to very low BET surface areas.

A further possibility for the catalyst preparation is the precipitation of lanthanum dihydroxychloride from a lanthanum chloride solution (Eq. (6)). The precipitated lanthanum hydroxychloride is calcined at 550 °C to yield the catalyst precursor lanthanum oxychloride (Eq. (7)) [12,13]:

$$LaCl_{3,aq} + \text{base} \rightarrow La(OH)_2Cl \quad (6)$$

$$La(OH)_2Cl \xrightarrow{550\,^\circ C,\,8\,h} LaOCl + H_2O \quad (7)$$

We have taken this approach using different organic bases for precipitation in order to prepare high surface area samples. The influence of the used base on the morphology and composition of the sample before and after chlorination is investigated. Furthermore, the catalytic performance of the prepared samples in oxyhydrochlorination is evaluated.

2. Experimental

2.1. Catalyst preparation

$LaCl_3$ catalysts were prepared in situ in an HCl flow from LaOCl precursors. The LaOCl precursors were prepared by precipitation at room temperature using ammonium hydroxide (NH_4OH), tetraethylammonium hydroxide (TEAOH, Merck, 20% aq. sol.), tetrapropylammonium hydroxide (TPAOH, Merck, 40% aq. sol.) or tetrabutylammonium hydroxide (TBAOH, Aldrich 99.9%, 20% aq. sol.) as base and a solution of lanthanum(III) chloride heptahydrate (99%, Merck) in ethanol (1 M). After drop-wise addition of the base to the solution, the suspension was stirred for 1 h to facilitate complete precipitation. The gel obtained after centrifugation was washed twice with excess of ethanol to remove the base. Finally, the gel was freeze dried and calcined at 550 °C using a temperature increment of 5 °C min^{-1} in a flow of synthetic air (200 ml min^{-1}) for 8 h. LaOCl was initially activated in He flow (40 ml min^{-1}) at 550 °C for 1 h. Subsequently, the material was converted to $LaCl_3$ in situ by reacting with HCl (20 vol.% HCl in He, total flow 50 ml min^{-1}) at 400 °C for 10 h.

The samples are denominated as LaOCl S1 to LaOCl S4 with the base used for precipitation in brackets.

2.2. Physicochemical characterization

The crystallographic structure of the LaOCl precursors and resulting $LaCl_3$ catalysts was determined by XRD with a Philips X'Pert Pro System (Cu Kα1-radiation, 0.154056 nm) at 40 kV/40 mA. The measurements were performed with a step scan of 0.017° min^{-1} from 10° to 60° 2θ and a time per step of 29.84 s.

The morphology and particle size of the LaOCl precursors and the chemical analysis by energy dispersive X-ray spectroscopy (EDX) were examined by scanning electron microscopy using a *JEOL* 500 SEM-microscope (accelerating voltage 20 kV). Before recording the SEM image, the sample was outgassed for 2 days at room temperature and sputtered with gold before collecting the images.

The specific surface area and pore volume were determined by nitrogen adsorption at 77 K using a PMI automated BET Sorptometer. The mesopore size distribution was obtained from the desorption branch of the isotherm using the Barret–Joyner–Halenda (BJH) method, the micropore volume was obtained from the desorption branch of the isotherm using the Horvath–Kawazoe (HK) method [14]. Prior to measurement, the LaOCl samples were outgassed in vacuum (10^{-3} Pa) at 250 °C for 2 h.

2.3. Catalytic tests

The in situ prepared $LaCl_3$ sample was tested in methane oxidative chlorination using a fixed-bed quartz tubular reactor charged with 250 mg of LaOCl precursor (0.63–1 mm size fraction). The temperature of the reactor oven was controlled by a thermocouple placed above the catalyst bed. The gas flows (CH_4, O_2, HCl, N_2, He) were controlled using digital mass flow meters (Bronkhorst).

The catalytic tests were performed in the temperature range 450–550 °C using 5 ml min^{-1} of the stoichiometric mixture CH_4:HCl:O_2:He:N_2 = 2:2:1:4:1. Helium was used as a diluent, and nitrogen as an internal standard. The reactor outlet was analyzed by an online Siemens Maxum Edition II gas chromatograph (GC). After analysis, the gases were passed through water and NaOH scrubbers to remove unreacted HCl. Gas lines of the setup were coated with glass lining and heated to 150 °C to prevent water condensation and corrosion.

The ability of the catalyst to accept chlorine was studied with temperature programmed chlorination experiments. A mixture of He:HCl (4:1; 50 ml min^{-1}) was passed over 250 mg of the sample while increasing the temperature from room temperature to 650 °C with 2 °C min^{-1}. The HCl uptake was monitored by GC analysis.

Table 1
Elemental composition of the LaOCl precursor and N_2 physisorption on catalyst precursors and the chlorinated material

Sample	Precursor					Chlorinated	
	La (mol%)	Cl (mol%)	C (wt.%)	BET area ($m^2\ g^{-1}$)	Pore volume ($cm^3\ g^{-1}$)	BET area ($m^2\ g^{-1}$)	Pore volume ($cm^3\ g^{-1}$)
S1 (NH_4OH)	26.7	24.2	0.02	21	0.063	<1	–
S2 (TEAOH)	26.7	16.1	0.89	125	0.377	6	0.028
S3 (TPAOH)	15.6	5.2	1.53	118	0.435	11	0.143
S4 (TBAOH)	30.6	15.1	0.78	78	0.360	3	0.036

3. Results

3.1. Physicochemical characterization

The N_2 physisorption results of the freshly prepared and chlorinated samples are summarized in Table 1. The samples precipitated with organic bases exhibit a higher BET surface area compared to the sample precipitated with ammonium hydroxide. The highest specific surface area was obtained with TEAOH as precipitating base. However, with increasing chain length of the alkyl group the specific BET area decreased.

The adsorption/desorption isotherms of all samples correspond to a type IV isotherm characterized by a hysteresis loop, generated by capillary condensation of the adsorbate in the mesopores. The hysteresis loop corresponds to the type H3 loop, which is observed with aggregates of plate-like particles giving rise to slit-shaped pores [15]. This is also confirmed by TEM measurements of LaOCl S2 (TEAOH) which showed agglomeration of plate-like primary particles with a median length of 200 and 45 nm thickness (see Fig. 2).

The different bases also influenced the pore size distribution as shown by the comparison of the BJH-plot for S1 (NH_4OH) and S4 (TBAOH) in Fig. 3. LaOCl S1 (NH_4OH) showed a pore size distribution with a main pore diameter of around 3.8 nm. Whereas, larger pores with a pore diameter around 10 nm were obtained by precipitation with organic bases. For LaOCl S4 (TBAOH), the pore size distribution reached a maximum of around 12.5 nm.

The XRD pattern of the LaOCl S1 (NH_4OH) samples is shown in Fig. 4. The diffraction pattern for tetragonal LaOCl was present in all samples according to the JCPDS-file 73-2063 of LaOCl. SEM photographs show also the agglomeration of the primary particles to much larger particles with an irregular shape and diameters between 3.5 and 25 μm in case of LaOCl S1 (NH_4OH). While the morphology was similar for all samples, the particle size reached up to 100 μm for the samples precipitated with organic bases. As example, the SEM photograph for the fresh LaOCl S2 (TEAOH) is shown in Fig. 5a.

In order to prepare $LaCl_3$, typically the most active form of the catalyst, the samples are activated and chlorinated with HCl for 10 h at 400 °C prior to the catalysis. After this procedure the specific surface area of all samples decreased. The specific surface area of S2 (TEAOH), for example, decreased from 125 $m^2\ g^{-1}$ for the catalyst precursor to 6 $m^2\ g^{-1}$ after 10 h of chlorination (see Table 1). This corresponds to about 5% of the original BET surface area. Fig. 6 shows that the chlorinated sample adsorbed a much lower amount of N_2 compared to the LaOCl precursor. The ratio between the area of hysteresis and the area below the adsorption line increased by a factor of 2.5 for the chlorinated form. This indicates that chlorination reduces the concentration of accessible micropores to a higher extent than for the mesopores. This effect was even more pronounced with S3 (TPAOH). After chlorination, 36% of the original mesopore volume and only 10% of the original micropore volume was retained. The reduction in specific surface area was observed for all samples.

The highest specific surface area after chlorination was observed for S3 (TPAOH). Around 9% of the BET surface area of the precursor were preserved indicating some stabilization during chlorination (see Table 1). The SEM photograph (Fig. 5b) clearly shows a further agglomeration of the particles after chlorination leading to particles size ranging from 5 to 210 μm.

The elemental composition of the synthesized LaOCl precursors was determined by EDX and is summarized in Table 1. It should be noted that the concentrations of lanthanum and chlorine do not correspond to pure stoichiometric LaOCl. Only the S1 sample precipitated with the inorganic base NH_4OH showed a La/Cl ratio of 1. The La/Cl ratio of the samples precipitated with organic bases ranged between 2 and 3. Together with the presence of carbon in these samples this deviation indicates that $La_2(CO_3)_3$ is present either on the surface or as bulk carbonate. To quantify this observation, the carbon content was determined by CHN analysis and is summarized in Table 1. The carbonate content decreases in

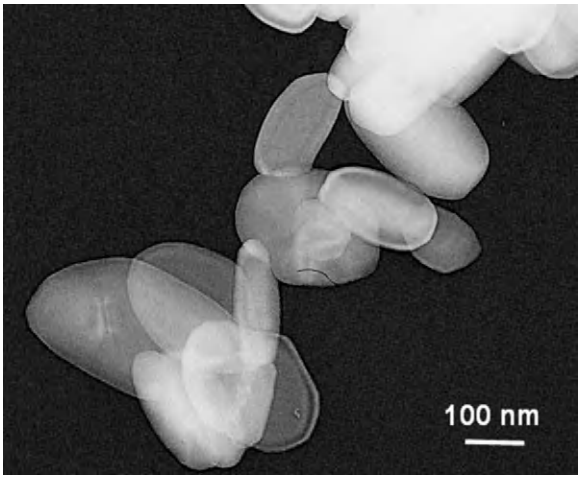

Fig. 2. TEM photograph of LaOCl S2 (TEAOH).

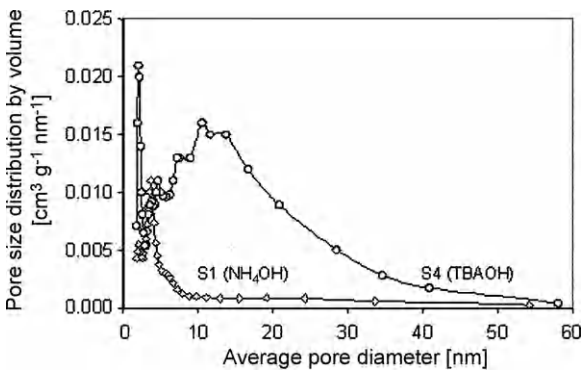

Fig. 3. Pore size distributions (BJH-plot) of (◇) LaOCl S1 (NH_4OH) and (○) LaOCl S4 (TBAOH).

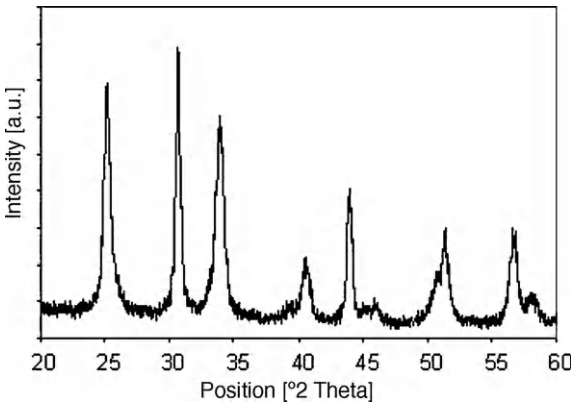

Fig. 4. XRD diffractogram of the LaOCl S1(NH_4OH).

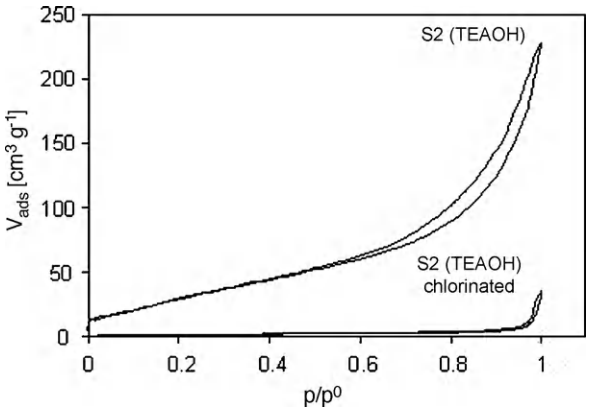

Fig. 6. N_2 adsorption/desorption isotherm of LaOCl S2 (TEAOH) precursor and chlorinated material.

the following sequence:

$$S3\,(TPAOH) > S2\,(TEAOH) > S4\,(TBAOH) > S1\,(NH_4OH) \quad (8)$$

The highest carbonate content was found in S3 (TPAOH), followed by S2 (TEAOH) which had a similar carbonate content as S4 (TBAOH). The lowest carbonate content was found S1 (NH_4OH).

3.2. Chlorination of the precursor

Full chlorination is essential for a highly active and selective catalyst, as lattice oxygen atoms on the surface are active for the catalytic destruction of chlorinated hydrocarbons [16–18]. In order to understand the kinetics of this process and to assure the completeness, the ability for HCl uptake was tested in temperature programmed chlorination. The results are compiled in Fig. 7. The total HCl uptake and the maximum temperature for HCl uptake varied between the different samples. The S3 (TPAOH) sample showed the highest HCl uptake of 0.0112 mol HCl g^{-1} with a maximum uptake at 287 °C (±5 °C), followed by S2 (TEAOH) with 0.0088 mol HCl g^{-1} uptake and a maximum at 231 °C (±5 °C). The most easily chlorinated catalyst was S4 (TBAOH) with a maximum uptake at 200 °C (±5 °C). The total uptake for this sample was 0.0076 mol HCl g^{-1}. The sample synthesized with NH_4OH possessed with 0.0064 mol HCl g^{-1} the lowest HCl uptake and also the highest maximum uptake temperature at 325 °C (±5 °C). However, it should be noted that the uptake does not correspond to a total chlorination, as exposure of the materials at the optimum chlorination temperature was too short. The HCl uptake of the different samples varies in the following sequence:

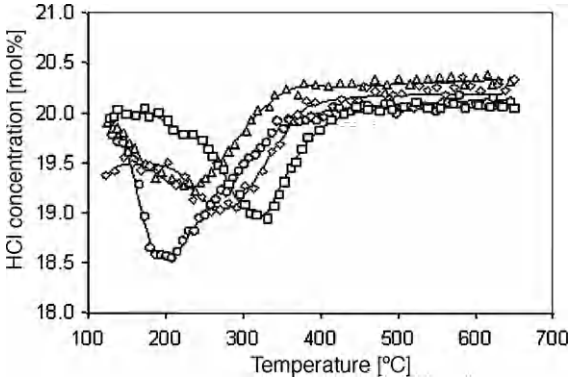

Fig. 7. Temperature programmed chlorination with 20 vol.% HCl and a temperature increment of 2 °C min^{-1}; (□) S1 (NH_4OH), (△) S2 (TEAOH), (◇) S3 (TPAOH), (○) S4 (TBAOH).

$$S3\,(TPAOH) > S2\,(TEAOH) > S4\,(TBAOH) > S1\,(NH_4OH) \quad (9)$$

As all samples contain a certain amount of lanthanum carbonate, a temperature programmed chlorination with pure lanthanum carbonate hydrate was performed. Activated in the same manner as LaOCl, it showed an optimum temperature for HCl uptake at around 440 °C (results not shown).

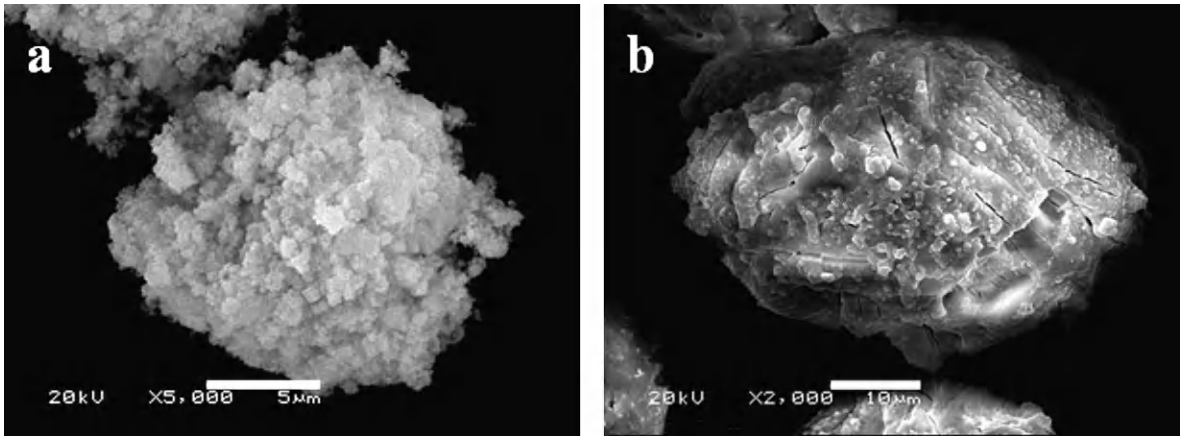

Fig. 5. (a and b) SEM photographs of LaOCl S2 (TEAOH) (a) precursor and (b) chlorinated at 400 °C for 10 h.

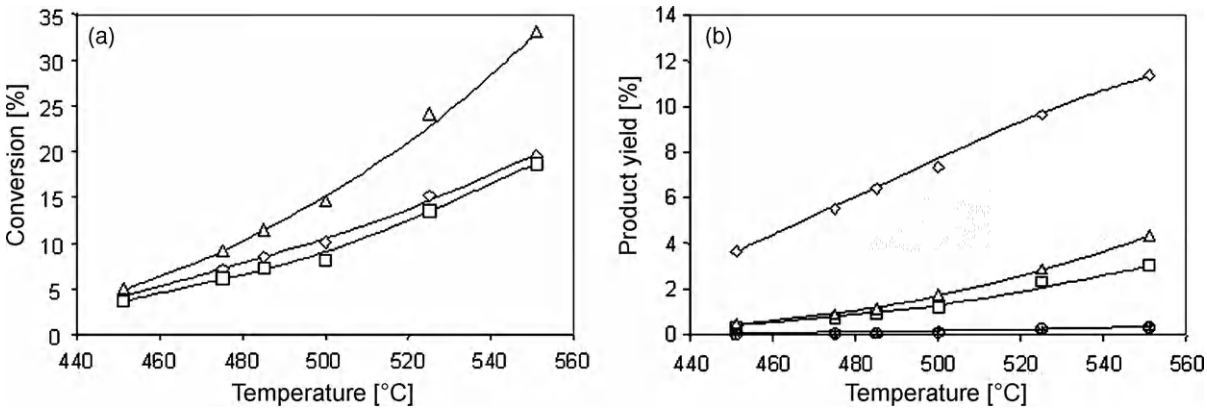

Fig. 8. (a) Reactant conversion over LaOCl S1 (NH_4OH) in the temperature range between 450 and 550 °C at constant space velocity with stoichiometric flow CH_4:HCl:O_2:He:N_2 = 2:2:1:4:1 ((◇) CH_4, (□) HCl, (△) O_2). (b) Product yields over LaOCl S1 (NH_4OH) in the temperature range between 450 and 550 °C at constant space velocity with stoichiometric flow CH_4:HCl:O_2:He:N_2 = 2:2:1:4:1 ((◇) CH_3Cl, (□) CH_2Cl_2, (○) $CHCl_3$, (△) CO, (✳) CO_2).

3.3. Catalytic conversion of methane

The reactant conversion in the temperature range from 450 to 550 °C over LaOCl S1 (NH_4OH) is shown in Fig. 8a. By increasing the temperature the methane conversion increased from 4.5% to 19.5%. At 450 °C the oxygen and hydrogen chloride conversion was equal to the methane conversion. However, the oxygen conversion showed a stronger increase with temperature than the methane conversion and reached 33% at 551 °C. The HCl conversion was slightly lower than the methane conversion and the increase parallels with the increase of the methane conversion in the whole temperature range. The distribution of the product yields in the same temperature range is shown in Fig. 8b. Methyl chloride was the main product formed in the whole temperature range and the yield increased with temperature from 3.6% to 11.5%. As by-products also carbon monoxide and methylene chloride were formed. The yield of carbon monoxide and methylene chloride increased with temperature, with the increase being more pronounced at higher temperatures. Chloroform and tetrachloromethane were formed only in negligible amounts, CO_2 was hardly detected.

The reactant conversion and product yields on methane conversion in the same temperature range over S3 (TPAOH), as example for an organic precipitated catalyst, are shown in Fig. 9a and b. The LaOCl S3 (TPAOH) material showed higher reactivity. Similar to LaOCl S1 (NH_4OH), the oxygen and hydrogen chloride conversion were equal to the methane conversion at 450 °C. The HCl conversion was always slightly lower than the methane conversion and the oxygen conversion showed a strong increase with temperature up to 88% at 555 °C. Over LaOCl S3 (TPAOH) methyl chloride was also the main product and reached a maximum yield of 17.1% at 500 °C. Carbon monoxide and methylene chloride yield strongly increased with temperature.

The catalysts precipitated with organic bases showed in general a higher activity for methane conversion compared to the catalyst precipitated with NH_4OH. The highest rate for methane conversion at 527 °C was obtained over S3 (TPAOH). This catalyst converted 1.1 μmol CH_4 g_{cat}^{-1} s^{-1}, whereas S1 (NH_4OH) converted at 527 °C only 0.68 μmol CH_4 g_{cat}^{-1} s^{-1}. The selectivity to methyl chloride of all studied catalysts was at the same methane conversion almost equal. The dependence of methyl chloride yield, the desired product, on methane conversion of all studied catalysts is provided in Fig. 10. The dashed line indicates the yield for 100% selectivity. At low methane conversion the yield towards methyl chloride increased with methane conversion. At higher methane conversion the increase of the methyl chloride yield slowed down or even decreased. It is important to note, that the data were collected at different reaction temperatures, thus we cannot speculate about the mechanism. However, the same trend of the methyl chloride yield with methane conversion indicates that the same active sites are present in all studied catalysts. The dependence of methylene chloride yield is shown in Fig. 11. The methylene chloride yield was for all samples in the same range and increased with increasing methane conversion. The increase is more pronounced at higher methane conversion.

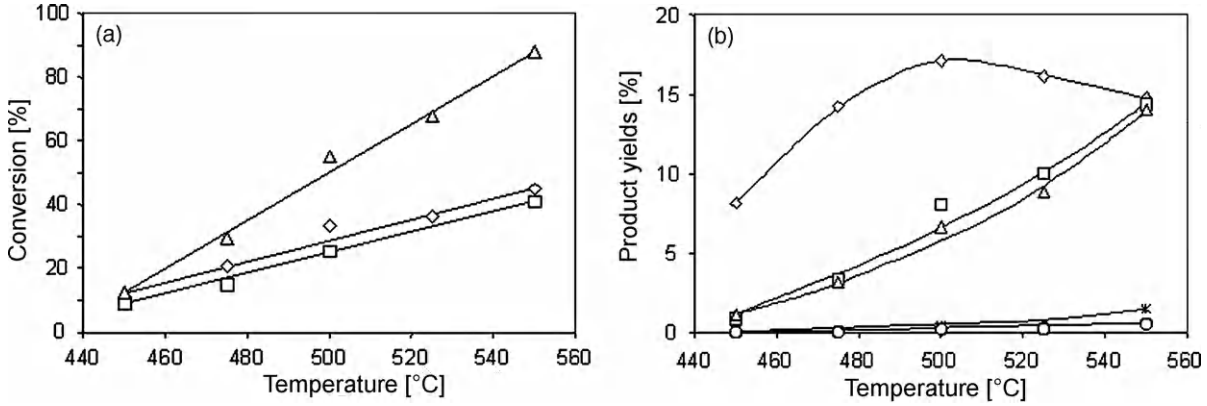

Fig. 9. (a) Reactant conversion over LaOCl S3 (TPAOH) in the temperature range between 450 and 550 °C at constant space velocity with stoichiometric flow CH_4:HCl:O_2:He:N_2 = 2:2:1:4:1 ((◇) CH_4, (□) HCl, (△) O_2). (b) Product yields over LaOCl S3 (TPAOH) in the temperature range between 450 and 550 °C at constant space velocity with stoichiometric flow CH_4:HCl:O_2:He:N_2 = 2:2:1:4:1 ((◇) CH_3Cl, (□) CH_2Cl_2, (○) $CHCl_3$, (△) CO, (✳) CO_2).

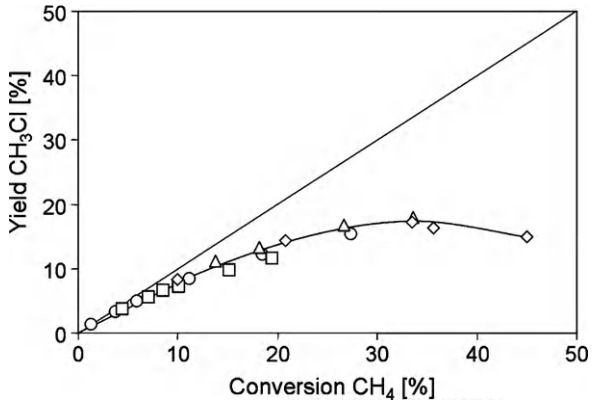

Fig. 10. Dependence of CH_3Cl yield on CH_4 conversion in the temperature range between 450 and 550 °C at a constant space velocity (CH_4:HCl:O_2:He:N_2 = 2:2:1:1:4:1); (□) S1 (NH_4OH), (△) S2 (TEAOH), (◇) S3 (TPAOH), (○) S4 (TBAOH), (—) 100% selectivity line.

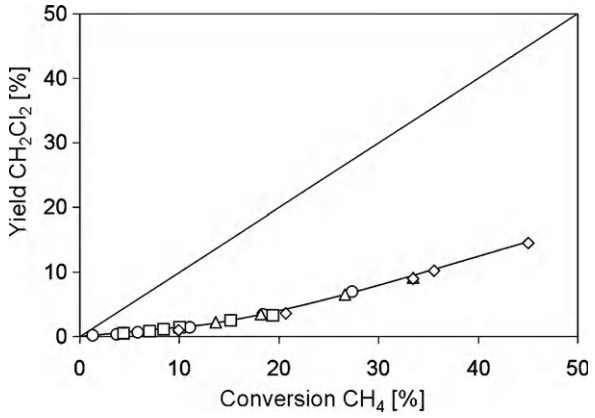

Fig. 11. Dependence of CH_2Cl_2 yield on CH_4 conversion in the temperature range between 450 °C and 550 °C at a constant space velocity (CH_4:HCl:O_2:He:N_2 = 2:2:1:1:4:1); (□) S1 (NH_4OH) (△) S2 (TEAOH), (◇) S3 (TPAOH), (○) S4 (TBAOH), (—) 100% selectivity line.

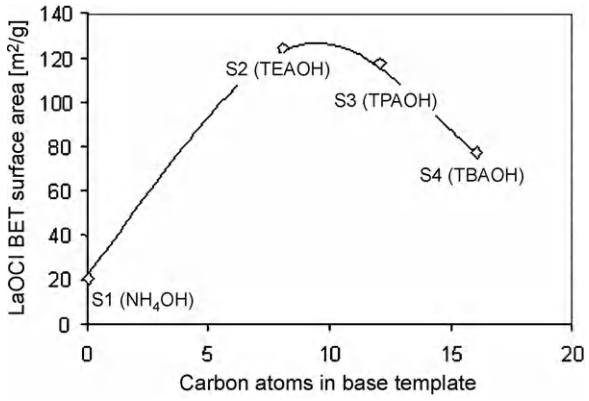

Fig. 12. Influence of the number of carbon atoms in the base template on LaOCl BET surface area.

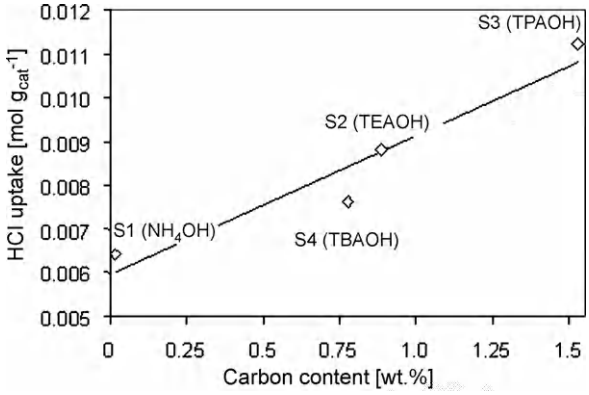

Fig. 13. Influence of the carbon content in the catalyst precursor on the HCl uptake (symbol) and linear fit (line) of $y = 0.003x + 0.006$; $R^2 = 0.9217$.

4. Discussion

The specific surface area and the pore size in precipitated chlorides depend in a complex way on the used bases and the drying methods employed. Compared with NH_4OH, organic bases led to a significantly higher specific surface area. This can be attributed on the one hand to the higher base strength, leading to a higher concentration of primary nuclei during the precipitation. It could also be speculated that the organic rest induces locally some sort of templating, such as the pore building action during the formation of zeolite gel precursors [19,20]. The fact that TEAOH led to the highest specific surface area points to the fact that latter influence is less important than the more rapid nucleation step. However there is also indication of pore collapse during calcination of $La(OH)_2Cl$ to LaOCl (see Fig. 12).

The composition of the surface obtained from the EDX analysis indicates a non-stoichiometric composition of the lattice for the organic precipitated samples. In general, a higher La/Cl ratio is observed on the samples precipitated with organic bases. In contrast, the NH_4OH precipitated sample shows a nearly ideal La/Cl ratio of 1.0. The deviation from the La/Cl ratio of 1.0 is attributed to traces of carbonates in the sample presumably on the catalyst surface. The higher La/Cl ratio of LaOCl samples precipitated with organic bases stems from the higher lanthanum carbonate content. Marsal et al. reported the excellent CO_2 absorption properties of LaOCl samples at low temperature and high humidity [10,21]. Thus, surface lanthanum carbonate can be generated by CO_2 adsorption from air. It should be pointed out that bulk carbonate can be formed in the organic precipitated samples by the adsorption of CO_2, which is a product of the decomposition of the amines occurring during the calcination treatment of the precipitated $La(OH)_2Cl$.

The variations in the specific surface area and the mesoporous structure influence also the chlorination behavior of the samples. Temperature programmed chlorination is used to monitor the chlorination ability of LaOCl to $LaCl_3$ (Eq. (10)).

$$LaOCl + 2HCl \rightleftharpoons LaCl_3 + H_2O \quad (10)$$

Simultaneously lanthanum dioxocarbonate which is present in the sample is also chlorinated with 6 mol HCl (Eq. (12)). Lanthanum dioxocarbonate is generated by the decomposition of lanthanum carbonate during the activation treatment in helium (Eq. (11)) [22].

$$La_2(CO_3)_3 \xrightarrow{\Delta T} La_2O_2CO_3 + 2CO_2 \quad (11)$$

$$La_2O_2CO_3 + 6HCl \rightarrow 2LaCl_3 + CO_2 + 3H_2O \quad (12)$$

Therefore, the HCl uptake is correlated with the carbonate content of the samples. Fig. 13 clearly shows the linear correlation between the HCl uptake and the carbon content of the sample, which represents the carbonate content. Lanthanum carbonate has

a maximum chlorination temperature of 440 °C and the LaOCl samples are commonly chlorinated at 400 °C. Thus, the lanthanum carbonate chlorination is slower compared to the LaOCl chlorination. However, a 10 h chlorination treatment is sufficient to chlorinate all present carbonates, because after such chlorination no remaining carbon was found by CHN analysis.

The HCl uptake is not only influenced by the carbonate content of the sample, but also by the specific area of the LaOCl precursor. The S1 (NH_4OH) catalyst which has the lowest BET surface area of all samples possesses also the lowest HCl uptake. The mesoporous structure of the organic precipitated samples facilitates the chlorination because HCl can easily penetrate the bulk of LaOCl via the pore structure. The S1 (NH_4OH) sample is chlorinated only via the outer surface and bulk chlorination takes place by oxygen diffusion to the surface. This explains also the higher optimum chlorination temperature of S1 (NH_4OH). Furthermore the S1 (NH_4OH) catalyst has an almost ideal LaOCl structure, which is more difficult to chlorinate compared to the disordered LaOCl structure of the organic precipitated samples.

The reactant conversion of S1 (NH_4OH) and S3 (TPAOH), showed that at low reaction temperature the methane, oxygen and hydrogen chloride conversion is equal. This indicates the stoichiometric conversion of methane and oxygen to methyl chloride and that the catalyst surface is regenerated with HCl according to Eq. (1). In agreement with our earlier finding, methyl chloride is formed as a primary product over $LaCl_3$-based catalysts [2,23]. Methyl chloride can either desorb from the surface or parts of the formed methyl chloride species can be retained on the surface. This leads to a catalytic pathway that favors the reaction of the strongly bound (partially chlorinated) methyl species with hydroxy groups formed during the initial step or with oxygen present in the sample. In addition to this pathway the re-adsorption of methyl chloride and additional chlorination or oxidation of the re-adsorbed species to CO takes place. The more pronounced increase of the oxygen conversion with increasing reaction temperature in Figs. 8a and 9a is, thus, attributed on the one hand to the further chlorination of methyl chloride to methylene chloride, which consumes hydrogen chloride and oxygen, while the methane conversion is not affected. On the other hand oxygen is also consumed due to the further oxidation of the chlorinated products to CO, while during the catalytic destruction of chlorinated products to CO, hydrogen chloride is released [12,16–18]. This explains the parallel increase of HCl conversion with methane conversion even though higher chlorinated products are formed.

The presence of the same active site in all samples is confirmed by the same correlation of methyl chloride selectivity with methane conversion, which is observed to lie almost along the same line for all samples. Thus, it is concluded that only the concentration of active sites increases compared to the $LaCl_3$ catalysts prepared by NH_4OH precipitation.

Also the porosity and morphology change by chlorination as shown by the N_2 physisorption results and SEM photographs of the chlorinated samples. The high BET surface area of the organic precipitated samples cannot be preserved during chlorination. In this process LaOCl samples are transformed to $LaCl_3$ and the structural information of the precursor is lost.

However, a direct relation exists between the specific surface area after chlorination and the CH_4 conversion as shown in Fig. 14. This trend clearly supports the conclusion that the oxyhydrochlorination of methane is a surface catalyzed reaction. It is interesting to note, however, that a direct correlation between the specific surface area of LaOCl and the specific surface area of the chlorinated catalyst does not exist. While the S3 (TPAOH) precursor does not have the highest BET surface area, it shows

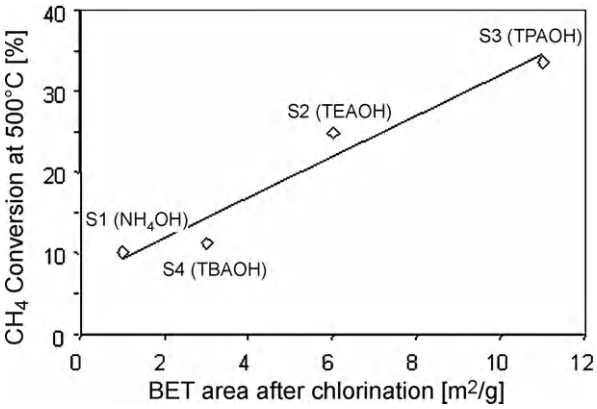

Fig. 14. Correlation of methane conversion at 500 °C with the BET surface area after chlorination (symbol) and linear fit (line) of $y = 2.53x + 6.69$; $R^2 = 0.9479$.

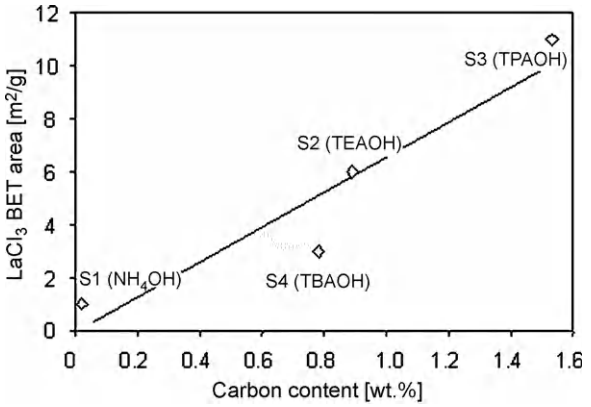

Fig. 15. Influence of the carbon content of the catalyst precursor on the $LaCl_3$ BET surface area (symbol) and linear fit (line) of $y = 6.63x - 0.09$; $R^2 = 0.891$.

the highest BET area after chlorination. The S3 (TPAOH) sample is characterized by the highest carbonate content of all prepared samples. As the LaOCl phase is faster chlorinated than lanthanum dioxocarbonate, the latter acts like a structural promoter and stabilizes the porous structure. In the final step lanthanum dioxocarbonate is then fully chlorinated, but the already converted $LaCl_3$ suffices to stabilize the pore structure better. This connection is shown in Fig. 15. The BET surface area after chlorination is influenced by the carbon content in the catalyst precursor.

5. Conclusion

Samples of LaOCl with high specific surface area can be prepared, using the organic bases as precipitating agents. During the chlorination treatment the specific surface area drastically decreases. The decrease of the specific surface area is influenced by the carbonate content of the catalysts. The chlorination of lanthanum dioxocarbonate proceeds more slowly than LaOCl, and thus lanthanum dioxocarbonate acts like a structural promoter during chlorination, stabilizing the BET surface area. Eventually the lanthanum dioxocarbonate is also fully chlorinated. The methane conversion shows a linear correlation with the specific surface area after chlorination, indicating that all site generated have identical catalytic properties. The LaOCl specific surface area and the carbon content influence also the chlorination behavior of the catalyst and results in a lower optimum temperature for the HCl uptake. High surface area samples have a higher HCl uptake because HCl can easily penetrate LaOCl through the pores.

Acknowledgments

The authors thank X. Hecht for BET measurements and M. Neukamm for SEM and EDX measurements. Thanks go also to A. Kastenmüller of the Institute of electron microscopy of Technischen Universität München for TEM measurements. The authors are also grateful to T. Tafelmeier and U. Ammari of the microanalytical laboratory at Technischen Universität München for determining the carbon content by CHN analysis. Partial financial support by The Dow Chemical Company is gratefully acknowledged.

References

[1] A.E. Schweizer, M.E. Jones, D.A Hickman, Oxidative halogenation of C1 hydrocarbons to halogenated C1 hydrocarbons and integrated processes related thereto, Dow Global Technologies Inc., Midland, MI, US 6,452,058 B1 (2002).
[2] E. Peringer, S.G. Podkolzin, M.E. Jones, R. Olindo, J.A. Lercher, Top. Catal. 38 (1–3) (2006) 211–220.
[3] S.G. Podkolzin, E.E. Stangland, M.E. Jones, E. Peringer, J.A. Lercher, J. Am. Chem. Soc. 129 (2007) 2569–2576.
[4] S.G. Podkolzin, O.V. Manoilova, B.M. Weckhuysen, J. Phys. Chem. B 109 (23) (2005) 11634–11642.
[5] O.V. Manoilova, S.G. Podkolzin, B. Tope, J.A. Lercher, E.E. Stangland, J.-M. Goupil, B.M. Weckhuysen, J. Phys. Chem. B 108 (40) (2004) 15770–15781.
[6] A.W.A.M. Van der Heijden, S.G. Podkolzin, M.E. Jones, J.A. Bitter, B.M. Weckhuysen, Angew. Chem. Int. Ed. 47 (27) (2008) 5002–5004.
[7] J. Hölsä, L. Niinisto, Thermochim. Acta 37 (2) (1980) 155–160.
[8] J. Hölsä, M. Lahtinen, M. Lastusaari, J. Valkonen, J. Viljanen, J. Solid State Chem. 165 (1) (2002) 48–55.
[9] J. Lee, Q. Zhang, F. Saito, J. Solid State Chem. 160 (2) (2001) 469–473.
[10] A. Marsal, G. Dezanneau, A. Cornet, J.R. Morante, Sens. Actuators B 95 (2003) 266–270.
[11] G. Dezanneau, A. Sin, H. Roussel, H. Vincent, M. Audier, Solid State Commun. 121 (2/3) (2002) 133–137.
[12] P.V. Klevtsov, C. R. Acad. Sci. Ser. III 266 (6) (1968) 385.
[13] A.W.A.M. van der Heijden, V. Bellière, L.E. Alonso, M. Daturei, O.V. Manoilova, B.M. Weckhuysen, J. Phys. Chem. B 109 (50) (2005) 23993–24001.
[14] G. Horvath, K. Kawazoe, J. Chem. Eng. Jpn. 16 (6) (1983) 470–475.
[15] K.S.W. Sing, D.H. Everett, R.A.W. Haul, L. Moscou, R.A. Pierotti, J. Rouquerol, T. Siemieniewska, Pure Appl. Chem. 57 (4) (1985) 603–619.
[16] P. Van der Avert, B.M. Weckhuysen, Angew. Chem. Int. Ed. 41 (24) (2002) 4730–4732.
[17] P. Van der Avert, B.M. Weckhuysen, Phys. Chem. Chem. Phys. 6 (22) (2004) 5256–5262.
[18] A.W.A.M. Van der Heijden, M. Garcia Ramos, B.M. Weckhuysen, Chem. Eur. J. 109 (1/2) (2007) 97–101.
[19] M. Elanany, B.L. Su, D.P. Vercauteren, J. Mol. Catal. A: Chem. 270 (1/2) (2007) 295–301.
[20] O.A. Fouad, R.M. Mohamed, M.S. Hassan, I.A. Ibrahim, Catal. Today 116 (1) (2006) 82–87.
[21] A. Marsal, E. Rossinyol, F. Bimbela, C. Tellez, J. Coronas, A. Cornet, J.R. Morante, Sens. Actuators B 109 (2005) 38–43.
[22] M. Hoang, A.E. Hughes, J.F. Mathews, K.C. Pratt, J. Catal. 171 (1997) 313–319.
[23] E. Peringer, M. Salzinger, M. Hutt, A.A. Lemonidou, J.A. Lercher, J. Catal., submission for publication.